STUDIES OF LOW-ENERGY HEAVY-ION REACTIONS AT LNL*

A.M. STEFANINI, D. ACKERMANN, L. CORRADI, J.H. HE

Istituto Nazionale di Fisica Nucleare, Laboratori Nazionali di Legnaro
I-35020 Legnaro, Padova, Italy

S. BEGHINI, G. MONTAGNOLI, F. SCARLASSARA

AND G.F. SEGATO

Dipartimento di Fisica, Universitá di Padova
and Istituto Nazionale di Fisica Nucleare
Sezione di Padova, I-35131, Padova, Italy

(Received November 21, 1994)

Recent experimental investigations on low-energy heavy-ion reaction dynamics performed at Legnaro are reviewed. A short description is given of the setup which enables the study of elastic scattering and of quasi-elastic transfer reactions, as well as of fusion reactions. After a brief hint on the perspectives in the field of multinucleon transfer, the main part of the lecture is dedicated to the fusion reactions for which recent developments, like the studies of barrier distributions and the theoretical approach using the Interacting Boson Model, have led to a renewed interest. Some results obtained by our group are presented for the systems $^{32}S + {}^{58,64}Ni$, $^{16}O + {}^{194}Pt$ (sensitivity to the target deformation) and $^{58}Ni + {}^{60}Ni$ (evidence for multiphonon excitation in subbarrier fusion).

PACS numbers: 25.70. -z, 25.70. Jj

1. Introduction

The dynamics of heavy-ion reactions at energies near and below the Coulomb barrier have been of widespread interest for around 15 years, both experimentally and theoretically. Various reviews of the many facets of

* Presented at the XXIX Zakopane School of Physics, Zakopane, Poland, September 5–14, 1994.

such collisions have been published recently [1–3], and a topical meeting has been dedicated to fusion reactions earlier this year [4]. The present lecture aims at giving a sufficiently complete overview of the activities in this field, which are going on at Laboratori Nazionali di Legnaro (LNL), with obvious references to the results of other groups.

After a short description of the experimental setups at LNL, which are being used for the investigation of scattering, few- and multi-nucleon transfer reactions and fusion processes, the remaining part of the lecture will be dedicated to this last kind of reactions, whose understanding is taking great benefit from very recent experimental and theoretical developments. We shall describe the "barrier distribution" method [5] for analyzing the fusion excitation functions and its applications to the cases of deformed nuclei, vibrational nuclei and to the never cleared up influence of nucleon transfer (in particular pair transfer) on the fusion cross sections. We shall also recall an interesting theoretical approach [6] which exploits the Interacting Boson Model for the description of subbarrier fusion.

2. Experimental setup

The experimental facility for the study of low-energy heavy-ion reaction dynamics at LNL is composed of different parts. There is a 110 cm diameter scattering chamber, connected to the beam line by a sliding seal which allows a rotation of 90°. Two main devices are attached to the chamber: the first one is an electrostatic beam deflector followed by a time-of-flight (TOF) energy (E) telescope, for the detection of fusion-evaporation residues at 0° and at other small angles. This setup has been in use for a few years and is described in Ref. [7]. The second device, very recently installed, is a TOF spectrometer with magnetic focussing through two pairs of quadrupole doublets; the TOF is measured between two micro-channel plate detectors (MCP) over a length of $\simeq$4 m. A split-anode ionization chamber is placed at the "focal plane", where the energy E and energy loss ΔE of the incoming ions are measured. The effective solid angle of this setup is $\simeq$4 msr, up to magnetic rigidities of 1.5 Tm; its design and construction has been inspired from a similar apparatus built at GSI some years ago [8]. Angular distributions can be measured in the range $\simeq 0° - 155°$.

The TOF spectrometer has been used so far only for test and calibration measurements: in particular, for the detection at 80° of beam-like fragments from the collision of ^{32}S on ^{208}Pb at 185 MeV, which had been already studied at LNL. The mass resolution is very good, *i.e.* $\Delta A/A = 1/110$, with reasonably flat acceptance curves (yield *vs.* field gradient) for the many quasi-elastic transfer channels observed. Thus, the device is a very promising and efficient tool for the study of such reactions, also considering the

fact that the superconducting booster ALPI, injected by our XTU Tandem, is beginning to deliver heavier and higher energy beams than available so far (we were limited to Nickel beams of $\simeq$280 MeV or lower). The TOF spectrometer will also be operated in kinematical coincidence with multi-wire parallel-plate avalanche counters placed inside the scattering chamber, with $X - Y$ readout. In this case, the first MCP will also be position-sensitive, and such a detector is being constructed. The kinematical coincidence is essential for obtaining higher mass resolution (up to $\Delta A/A = 1/250$) as well as good Q-value resolution for *e.g.* elastic scattering measurements.

We shall not discuss here the recent results we obtained in the study of few- and multi-nucleon transfer reactions (see *e.g.* [9]), rather the rest of this lecture will be dedicated to fusion. We have dedicated a lot of work to the study of the role of angular momentum in subbarrier fusion, and recently a series of systems with different mass asymmetries in the entrance channel has been investigated; they are ^{58,64}Ni + ^{64}Ni, ^{28}Si + ^{94,100}Mo and ^{16}O + ^{112}Cd. The results on this last one have already been published [10], and all of them are the subject of another lecture at this School, given by D. Ackermann.

3. Fusion reactions and barrier distributions

When one performs measurements of fusion cross sections around and below the Coulomb barrier, one finds typical situations like that illustrated in Fig. 1 (left panels) for the two systems ^{32}S + ^{58,64}Ni we studied some years ago [11]. The cross sections are much larger than the one-dimensional tunnelling limits at subbarrier energies, and the enhancements are isotope-dependent; also, simple (as in this case) or complex coupled-channel (CC) calculations are able, by a suitable choice of one or a few parameters, of reproducing the excitation functions. Problems are anyway found for heavier systems, but even for the S + Ni cases we are led to ask ourselves some questions: are the data actually telling us that the essential difference between ^{32}S + ^{58}Ni and ^{32}S + ^{64}Ni is the presence of the neutron-pair transfer channel with positive Q-value in the latter system ? or are we forcing the data to tell us what we would like to find out, thus missing the real degrees of freedom which drive fusion in the two cases ? Of course in general one has to rely on additional observables: partial-wave cross sections, elastic and inelastic scattering, one- and few-nucleon transfer yields. But integral fusion cross sections are enhanced by *any* channel one couples in, so that drawing definite conclusions simply by a consideration of the apparently featureless excitation functions may be dangerous.

However, a step forward was taken with the introduction of the "experimental barrier distribution" method [5, 12] which pointed out how the

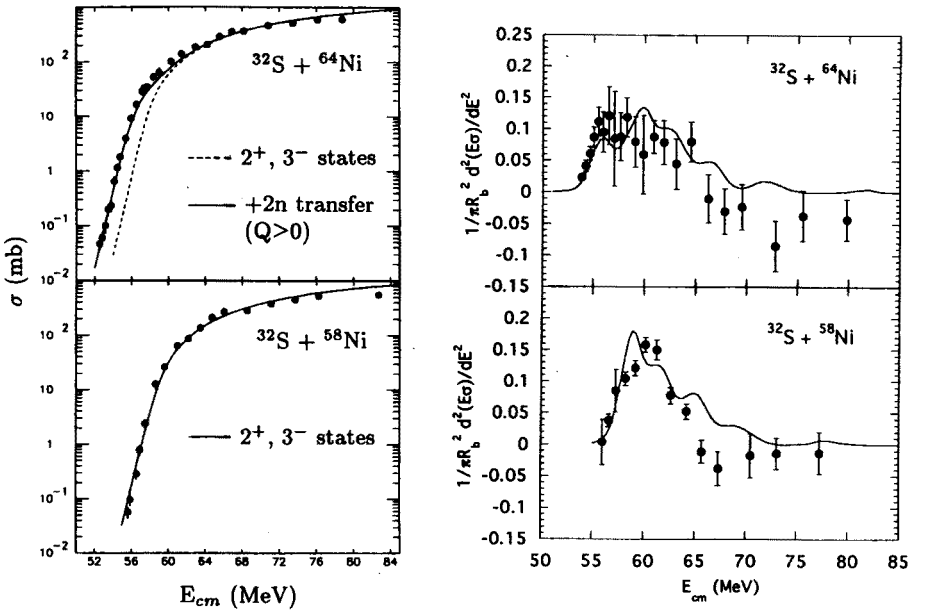

Fig. 1. Fusion excitation functions for $^{32}S + ^{58,64}Ni$ compared with simple *CC* calculations (left); barrier distributions extracted from the data compared with the same *CC* predictions (right).

distribution of fusion barriers, originating from channel couplings, can be obtained directly from the excitation functions. It was shown that from sufficiently accurate data one can extract distributions which frequently display a characteristic "fingerprint" of the type of couplings involved. The barrier distribution interpretation of heavy-ion fusion is described in detail elsewhere [5, 12]; here it is only necessary to recall that the second derivative of the excitation function $d^2(E\sigma)/dE^2$ is simply related to the *mean* barrier distribution $D(E)$, *i.e.* to the *true* distribution $D(B)$ originating from channel couplings, smoothed by a tunnelling factor. This picture is strictly valid in the adiabatic limit, *i.e.* when neglecting the excitation energies, because only in that case are the coupled equations simply solved and give rise to a manifold of barriers, each of which has its specific weight. When one has non-negligible, but small, excitation energies, one can show that the positions and relative weights of the adiabatic barriers are slightly changed, but the overall picture is still valid.

Now, how does one obtain "experimentally" the second derivative of the excitation function ? One method has been mostly exploited so far: *i.e.* for a set of fusion cross sections measured with a fixed energy spacing one

can approximate the derivative by the point-difference formula [12]

$$\frac{d^2(E\sigma)}{dE^2} = \frac{2(E\sigma)_n - (E\sigma)_{n+1} - (E\sigma)_{n-1}}{\Delta E^2}. \tag{1}$$

If the statistical errors are $\delta\sigma_n = f\sigma_n$ (fixed fractions of the cross sections), one has

$$\delta\left(\frac{d^2(E\sigma)}{dE^2}\right) \simeq \frac{\sqrt{6} f E\sigma}{\Delta E^2}. \tag{2}$$

The errors increase as the cross sections increase (and these change by orders of magnitude in the vicinity of the barrier), so that one expects more poorly defined distributions for energies higher than the barrier; the same is true if ΔE is "too small", but it has to be small enough to resolve any interesting structure. Anyway no fine structure on a scale $\Delta E \leq 0.56\hbar\omega \simeq 2-3$ MeV should show up due to the smearing of the barrier distributions introduced by tunnelling effects [5, 12] (here $\hbar\omega$ measures the thickness of the barrier). One also notices that systematic errors in the cross sections, or small errors in the overall energy scale, are likely to influence only a little the extracted barrier distributions; but relative cross sections must be measured very accurately.

The barrier distributions obtained this way for the $^{32}S + {}^{58,64}Ni$ systems are shown in the right panels of Fig. 1 together with the corresponding theoretical predictions which fit the excitation functions rather well. The distribution is wider in the case of the ^{64}Ni target and the agreement with theory is satisfactory, but the errors are large (these are old data which have been reanalyzed recently) so that no definite conclusion can be drawn. For $^{32}S + {}^{58}Ni$ the uncertainties are smaller, and the low-lying inelastic excitations in both nuclei can be actually considered to be the only important degrees of freedom for subbarrier fusion, as the *CC* calculations do reproduce the barrier distribution besides the fusion cross sections.

More characteristic distributions are predicted when one deals with deformed nuclei: Fig. 2 shows, for the collision of a spherical projectile with a prolate target, the peculiar and very different barrier distributions one expects [13] for different signs of β_4, the hexadecapole deformation parameter. Subbarrier fusion is very sensitive to the deformation parameters of the colliding nuclei: but are such predictions corroborated by experimental data? The answer is yes, as it is shown in Fig. 3 where the barrier distributions obtained by the Canberra group [14] are displayed for the two cases $^{16}O + {}^{186}W$ ($\beta_2 = 0.30$, $\beta_4 = -0.02$) and $^{16}O + {}^{154}Sm$ ($\beta_2 = 0.30$, $\beta_4 = +0.05$). The curves result from optimum fits to the excitation functions with the quoted deformation parameters.

There has been a recent novel approach to the problem of subbarrier fusion; in a series of papers Balantekin *et al.* [6] have used the Interacting

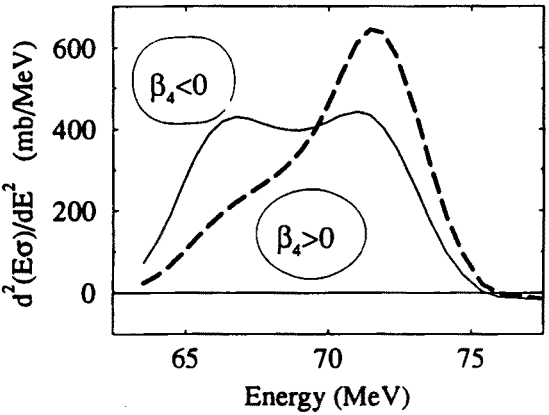

Fig. 2. Physical shapes and barrier distributions for different signs of β_4 (from Ref. [13]).

Boson Model (IBM) [15] to describe the structure of the colliding nuclei, and a Green's function technique to include couplings to all orders. This method has the advantage of avoiding the numerical complications needed for directly solving the coupled Schroedinger equations, and of being easily applied to transitional nuclei which fall between the SU(3) (rotational) and SU(5) (vibrational) limits, and for which a geometrical picture using shape parameters is often difficult. Fig. 4 (left) shows the effect of quadrupole coupling in deformed nuclei (with β_4 set to zero) for the case of prolate, oblate and γ-unstable shapes: in particular one notices that prolate and γ-unstable shapes can produce very similar excitation functions, and in such cases only a determination of the corresponding barrier distributions (very different from each other) may discriminate between the two shapes.

Balantekin *et al.* [6] point out that transitional nuclei may exhibit sharp changes in the barrier distribution as a consequence of shape-phase transitions. This is the case of the famous prolate-oblate shape transition in the Os-Pt mass region: Fig. 4 (right) shows the predicted fusion excitation functions and barrier distributions for the reactions $^{16}O + {}^{192}Os$ (prolate, with negative β_4) and $^{16}O + {}^{194}Pt$ (oblate, also with negative β_4). The effect of shape change is clearly visible in the very different barrier distributions, and we decided to check the situation experimentally. Preliminary results have already been obtained for the ^{194}Pt target, while the experiment with ^{192}Os will be performed soon. The evaporation-residue cross sections and the extracted barrier distribution for $^{16}O + {}^{194}Pt$ are shown in Fig. 5 together with the IBM predictions [6, 16].

Compound nucleus deexcitation by fission competes successfully with light particles evaporation already at energies slightly above the barrier; therefore the measured evaporation residue (ER) yields largely underesti-

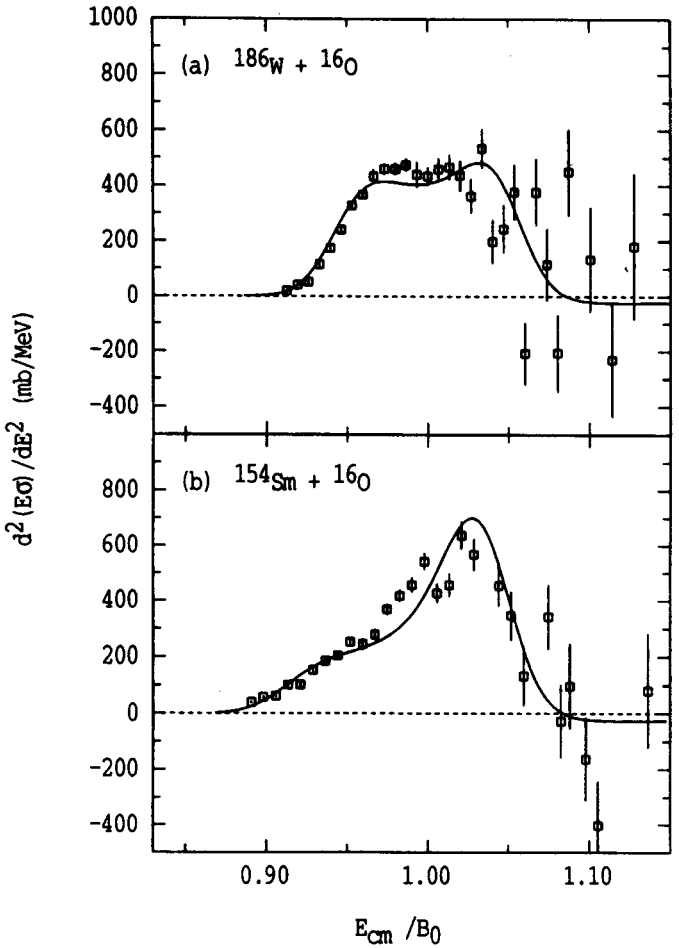

Fig. 3. Experimental barrier distributions for $^{16}O + ^{186}W$, ^{154}Sm plotted vs. the energy relative to the average barrier B_0; see text for details (taken from Ref. [14]).

mate the total fusion cross sections. We have estimated the fission cross sections by standard statistical model calculations, and by subtracting that contribution from the IBM prediction of the total fusion yield we get a reasonable agreement with the ER data above the barrier. Below the barrier the agreement is already good. Turning now to the barrier distribution (lower panel), one sees that the data display the characteristic feature predicted for the oblate nucleus ^{194}Pt, *i.e.* the distribution rises sharply below the barrier and then falls off more gently at higher energies. The missing fission cross section is probably responsible for the systematic disagreement one notices above the peak of the distribution. I stress again anyway the preliminary character of the data.

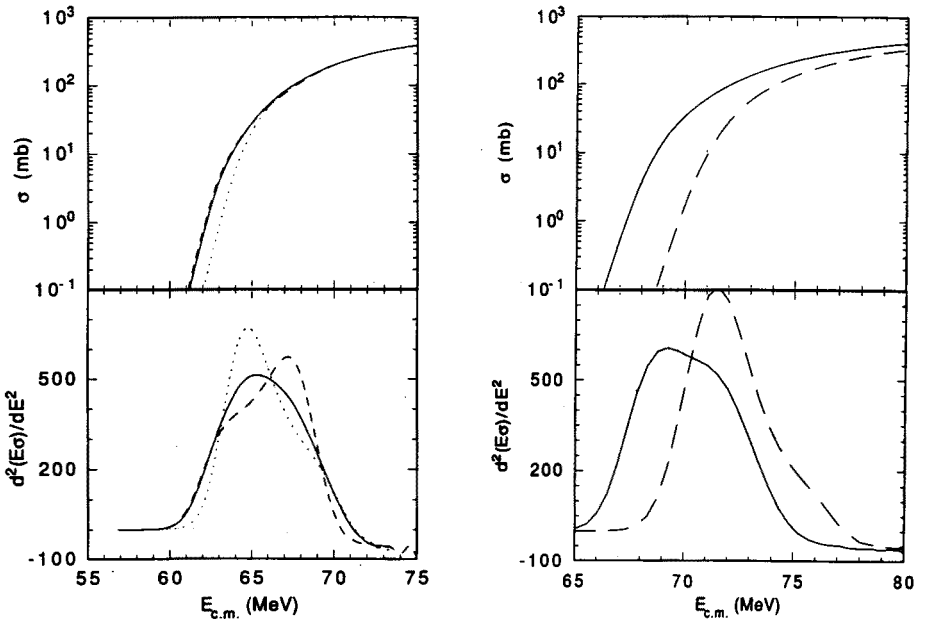

Fig. 4. Left: predicted effects of quadrupole couplings in deformed nuclei within the IBM approach [6], with prolate (dashed line), oblate (dotted line) and γ-unstable (solid line) shapes. Right: calculated excitation functions and barrier distributions for $^{16}O + ^{192}Os$ (solid line) and ^{194}Pt (dashed line) [6].

So far for deformed nuclei, and you see that there are quite interesting developments going on; we shall dedicate some time now to the longstanding problem of identifying the role of nucleon transfer in subbarrier fusion, which can hardly be disentangled from the concurrent effects of low-lying surface vibrations.

4. The fusion of $^{58}Ni + ^{60}Ni$

There is a particular case of nucleon transfer, where one can hope to identify its effect from the characteristic barrier distribution it produces: this is the elastic transfer of one or more nucleons. The fact that it has zero Q-value (the adiabatic limit) should make it possible to observe a a roughly symmetric distribution [17] with two peaks, one on each side of the original uncoupled Coulomb barrier, provided it is the dominant effect. For this reason we decided to investigate the system $^{58}Ni + ^{60}Ni$ where the elastic transfer of a neutron pair might produce such a structure.

The experiment was recently performed at LNL [18] and the results are shown in Fig. 6. The fusion excitation function is shown in the upper panel, where the energy scale is corrected for the target thickness, and

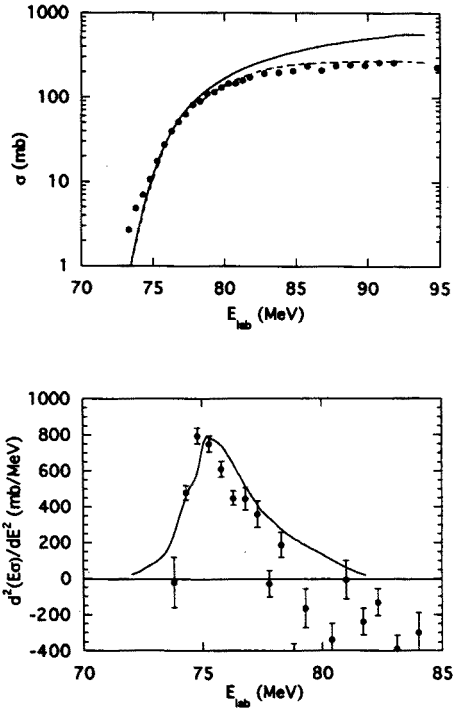

Fig. 5. Upper panel: preliminary data on evaporation residue cross sections in $^{16}O + {}^{194}Pt$, compared with the IBM predictions [6, 16]: the solid line is the calculated total fusion cross section, from which the fission cross section has been subtracted (dashed line, see text). Lower panel: the corresponding experimental and theoretical barrier distributions.

the target isotopic impurities are also taken into account. The (shown) statistical errors do not exceed the symbol size and are 2–3% for the higher and intermediate energies and increase to $\simeq$ 10% for the lowest ones. More details on the experiment can be found in the original paper [18]. The second derivative (lower panel) was extracted using the point-difference formula and it shows a rather interesting shape, since two large and very well resolved bumps of roughly equal weight show up, one on each side of the unperturbed barrier (100.9 MeV according to Ref. [19]). One is led to associate this immediately with the transfer of a neutron pair as described above. This would, however, be incorrect because one has to calculate firstly possible single and multiple phonon effects which are known to be important in the Nickel isotopes [20]. Also, there exists another smaller structure (a third bump) in the distribution at a lower energy, without whose presence the cross section itself would be much smaller at subbarrier energies.

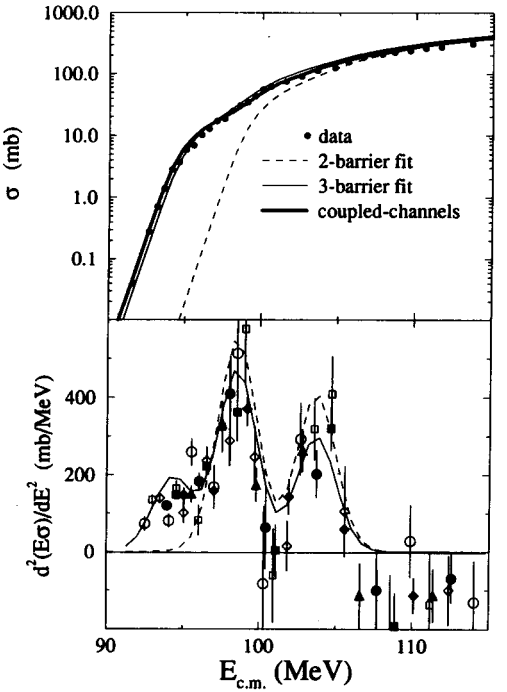

Fig. 6. Upper panel: the experimental fusion excitation function for ^{58}Ni+^{60}Ni is compared with phenomenological two-barrier and three-barrier fits and also with the full CC calculations described in the text. Lower panel: the "experimental barrier distribution" compared with the phenomenological fits.

As the elastic transfer of a neutron pair can produce only two barriers, let us consider the couplings to low-lying surface vibrations. The 2^+ single-phonon state has roughly the same energy in both nuclei (1.332 MeV in ^{60}Ni and 1.454 MeV in ^{58}Ni), so that the coupling to these two channels may be replaced by a single effective channel [21]. Two phonons are contained in three types of channels, *i.e.* the double-phonon excitations in each nucleus $|20\rangle$ and $|02\rangle$ and the mutual excitation of the single-phonon states $|11\rangle$. In both ^{58}Ni and ^{60}Ni, 0^+, 2^+ and 4^+ triplets exist with about twice the energy of the lowest 2^+ state but some of the γ-transitions deexciting them are unknown and others do not satisfy the vibrational limit too well [22]. We shall, however, for simplicity consider these states to be degenerate (with twice the average single-phonon energy) and to satisfy vibrational couplings. In this way we may perform a calculation with a single coupling parameter and all the two-phonon states may again be replaced by a single effective channel. Then, we may readily introduce three-phonon channels

of the form $|21\rangle$ and $|12\rangle$ *i.e.* by mutual excitation of the double and single phonon states and we may also clearly generate a four-phonon channel of the form $|22\rangle$, *i.e.* the mutual excitation of the two-phonon states.

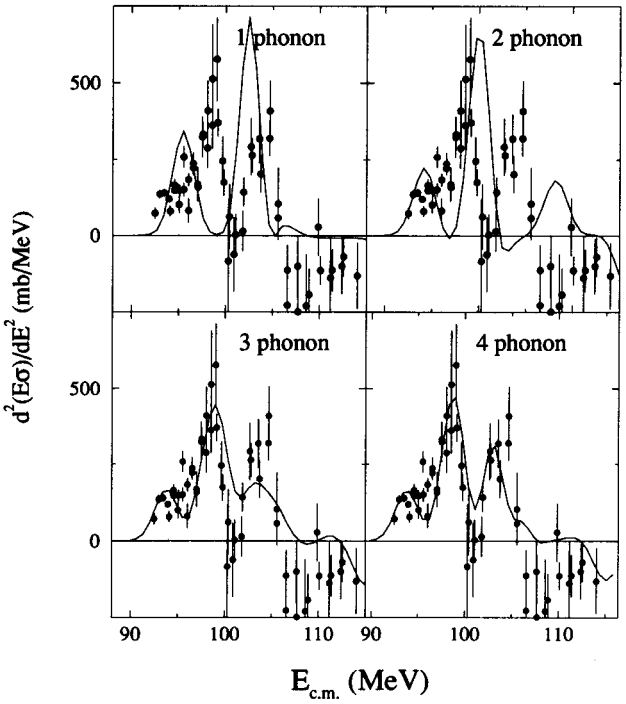

Fig. 7. The barrier distribution of ^{58}Ni+^{60}Ni is compared with *CC* calculations in the one-, two-, three- and four-phonon-channel spaces generated by considering up to mutual double excitations.

Fig. 7 shows the *CC* calculations of $d^2(E\sigma)/dE^2$ for the full 4-phonon-channel space and for truncations down to the 1-phonon level. Since the full space leads to quite large calculations, the isocentrifugal approximation was employed. The calculations are otherwise exact and take full account of the finite excitation energies. They also include Coulomb excitation and use an ingoing-wave boundary condition (IWBC). Essentially, two parameters were used: the "unperturbed" barrier height of 99.8 MeV and the r.m.s. value of the phonon deformation parameter $\langle\beta_2^2\rangle^{1/2} = 0.26$, *i.e.* somewhat larger than the value (0.21) obtained from $B(E2)$ values and deformation lengths [22]. More details on these calculations can be found elsewhere [18, 23]. The qualitative structure of the CC calculations changes as one increases up to the full space described above, though there is relatively little change between the 3- and 4-phonon spaces. While the 2- and 1-phonon spaces

clearly fail in describing the barrier distribution, the 4-phonon calculation gives an excellent fit to the data. The same full calculation produces the thick solid curve in Fig. 6 (upper panel), which gives a good fit to the measured excitation function.

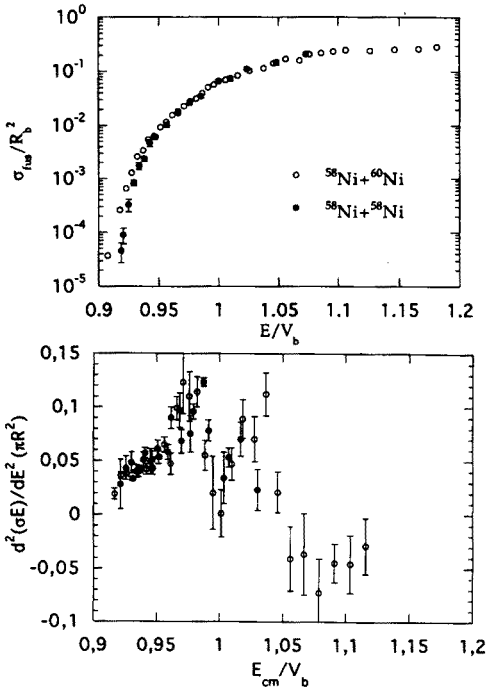

Fig. 8. Comparison of the ^{58}Ni+^{60}Ni and ^{58}Ni+ ^{58}Ni fusion excitation functions (upper panel) and barrier distributions (lower panel). For ^{58}Ni+ ^{58}Ni the errors are derived from those in Ref. [24], by subtracting the quoted systematic uncertainties.

What about the possible effects of neutron pair transfer ? It is true that the data are already extremely well fitted without inclusion of neutron-transfer channels, but this is not a good argument in itself for ignoring these effects. We can try to get some idea of their possible importance by comparing the ^{58}Ni + ^{60}Ni data with the older fusion data for ^{58}Ni + ^{58}Ni [24]. The phonon couplings here are almost identical and so any differences must come from transfer channels, since no adiabatic transfer channels are available in the symmetric system (all neutron transfer channels have negative Q-values). Fig. 8 shows the comparison, where reduced excitation functions are displayed (upper panel), and the barrier distributions are also plotted vs. the energy relative to the barrier (lower panel). One can see that within the experimental uncertainties and the more limited energy range measured for the symmetric system, the barrier distributions are very

similar, strongly suggesting that transfer effects are small and giving a very satisfactory confirmation of the dominance of surface vibrations. In particular the low-energy bump also exists in ^{58}Ni + ^{58}Ni. The relative cross section enhancement for ^{58}Ni + ^{60}Ni, present only at low energies, may qualitatively indicate that neutron transfer becomes important only well below the barrier.

Grateful thanks are due to Neil Rowley for his friendly collaboration and for performing the CC calculations for ^{58}Ni + ^{60}Ni. We also like to acknowledge the participation in the measurements at LNL of other colleagues: P. Bednarczyk, C. Petrache, P. Spolaore, D.R. Napoli, H.Q. Zhang, L. Mueller, C. Signorini, F. Soramel.

REFERENCES

[1] K.E. Rehm, *Annu. Rev. Nucl. Part. Sci.* **41**, 429 (1991).
[2] R. Vandenbosch, *Annu. Rev. Nucl. Part. Sci.* **42**, 447 (1992).
[3] W. Reisdorf, *J.Phys. G* **20**, 1297 (1994).
[4] Proc. Int. Workshop on Heavy-Ion Fusion Reactions, Padova (Italy), May 25-27, 1994, eds. A.M.Stefanini *et al.*, World Scientific, Singapore, in press.
[5] N. Rowley, G.R. Satchler, P.H. Stelson, *Phys. Lett.* **B254**, 25 (1990).
[6] A.B. Balantekin *et al.*, *Phys. Rev.* **C46**, 2019 (1992); **C48**, 1269 (1993); **C49**, 1079 (1994).
[7] S. Beghini *et al.*, *Nucl. Instr. Meth.* **A239**, 585 (1985).
[8] R. Bass *et al.*, *Nucl. Instr. Meth.* **130**, 125 (1975).
[9] L. Corradi *et al.*, *Z. Phys.* **A346**, 217 (1993); L. Corradi *et al.*, *Phys. Rev.* **C49**, R2875 (1994).
[10] D. Ackermann *et al.*, *Nucl. Phys.* **A575**, 374 (1994).
[11] A.M. Stefanini *et al.*, *Nucl. Phys.* **A456**, 509 (1986).
[12] N. Rowley, *Nucl. Phys.* **A538**, 205c (1992).
[13] N. Rowley, Ref. [4], in press.
[14] R.C. Lemmon *et al.*, *Phys. Lett.* **B316**, 32 (1993).
[15] F. Iachello, A. Arima, *The Interacting Boson Model*, Univ. Press, Cambridge 1987.
[16] S. Kuyucak, J. Bennett, private communication.
[17] N. Rowley, I.J. Thompson, M.A. Nagarajan, *Phys. Lett.* **B282**, 276 (1992).
[18] A.M. Stefanini *et al.*, *Phys. Rev. Lett.*, in press.
[19] L.C. Vaz, J.M. Alexander, G.R.Satchler, *Phys. Rep.* **69**, 373 (1981).
[20] H. Esbensen, S. Landowne, *Phys. Rev.* **C35**, 2090 (1987).
[21] A.T. Kruppa *et al.*, *Nucl. Phys.* **A560**, 845 (1993).
[22] M.M. King, *Nucl. Data Sheets* **69**, 1 (1993); L.K. Peker, *Nucl. Data Sheets* **61**, 189 (1990).
[23] A.T. Kruppa, N.Rowley, in progress.
[24] M. Beckerman *et al.*, *Phys. Rev.* **C23**, 1581 (1981).